

Hypocrellin B-loaded, folate-conjugated polymeric micelle for intraperitoneal targeting of ovarian cancer in vitro and in vivo

Jie Li^{1,2} | Shu Yao^{1,2} | Kai Wang³ | Zaijun Lu³ | Xuantao Su⁴ | Li Li^{1,2} | Cunzhong Yuan² | Jinbo Feng² | Shi Yan² | Beihua Kong^{1,2} | Kun Song^{1,2} 

¹Department of Obstetrics and Gynecology, Qilu Hospital, Shandong University, Jinan, China

²Gynecology Oncology Key Laboratory, Qilu Hospital, Shandong University, Jinan, China

³Department of Chemistry and Chemical Engineering, Shandong University, Jinan, China

⁴Department of Biomedical Engineering, School of Control Science and Engineering, Shandong University, Jinan, China

Correspondence

Kun Song, Department of Obstetrics and Gynecology, Qilu Hospital, Shandong University, Jinan, China.
Email: songkun2001226@sdu.edu.cn

Funding information

The National Science Foundation of China (Grant/Award Number: '81172488'), National Science Foundation of Shandong Province (Grant/Award Number: 'ZR2016HB14')

Photodynamic therapy (PDT) is considered an innovative and attractive modality to treat ovarian cancer. In the present study, a biodegradable polymer poly (ethylene glycol) (PEG)-poly (lactic acid)(PLA)-folate (FA-PEG-PLA) was prepared in order to synthesize an active-targeting, water-soluble and pharmacomodulated photosensitizer nanocarrier. Drug-loading content, encapsulation efficiency, in vitro and in vivo release were characterized, in which hypocrellin B (HB)/FA-PEG-PLA micelles had a high encapsulation efficiency and much slower control release for drugs compared to free drugs ($P < .05$). To evaluate the targeting ability of the HB/FA-PEG-PLA micelles, a cellular uptake study in vitro was carried out, which showed significantly enhanced uptake of HB/FA-PEG-PLA micelles in SKOV3 (FR+) compared to A2780 cancer cells (FR-). The enhanced uptake of HB/FA-PEG-PLA micelles to cancer cells resulted in a more effective post-PDT killing of SKOV3 cells compared to plain micelles and free drugs. Binding and uptake of HB/FA-PEG-PLA micelles by SKOV3 cells were also observed in vivo after ip injection of folate-targeted micelles in tumor-bearing ascitic ovarian cancer animals. Drug levels in ascitic tumor tissues were increased 20-fold ($P < .001$), which underscored the effect of a regional therapy approach with folate targeting. Furthermore, the HB-loaded micelles were mainly distributed in kidney and liver (the main clearance organs) in biodistribution. These results showed that our newly developed PDT photosensitizer HB/FA-PEG-PLA micelles have a high drug-loading capacity, good biocompatibility, controlled drug release, and enhanced targeting and antitumor effect, which is a potential approach to future targeting ovarian cancer therapy.

KEYWORDS

folate, intraperitoneal, nanoparticle, ovarian cancer, tumor targeting

1 | INTRODUCTION

Ovarian cancer is the leading cause of all gynecological malignancies. Late-stage patients have a 5-year survival rate of only 30%.¹

However, routine treatments do not significantly improve the prognosis of patients; new treatments must be explored to enhance the treatment efficiency of ovarian cancer. Photodynamic therapy (PDT) is considered an innovative modality to treat ovarian cancer.² Hypocrellin B (HB) is a good potential well-known second-generation photosensitizer, isolated from natural fungus sacs of *Hypocrella*

Li and Yao contributed equally to this work.

This is an open access article under the terms of the Creative Commons Attribution-NonCommercial License, which permits use, distribution and reproduction in any medium, provided the original work is properly cited and is not used for commercial purposes.

© 2018 The Authors. *Cancer Science* published by John Wiley & Sons Australia, Ltd on behalf of Japanese Cancer Association.

bambusae growing in the north-western region of Yunnan Province in China. Hypocrellin has advantages of high quantum yields of singlet oxygen, strong photogeneration of anion radicals in deoxygenated media, low dark toxicity, quick clearance from normal tissue and availability in a pure, monomeric form. Therefore, hypocrellin has been widely used in photodynamic therapy as a photosensitizer. Photodynamic therapy with HB or HB derivatives has been shown to have antitumor activity through induction of tumor cell apoptosis and inhibition of cell viability from several studies. An ideal photosensitizer should have such characteristics as better selectivity for tumor tissue, and higher photocytotoxicity with lower cytotoxicity under dark conditions. However, HB is hydrophobic; hence, it concentrates in the liver and spleen, not the targeted foci. Therefore, there is a need to develop an alternative formulation of HB with good aqueous solubility and high selectivity.

Nano-sized delivery systems such as polymer carriers,³ liposomes,⁴ micelles^{5,6} and nanogels⁷ have recently been widely used. They have passive targeting characteristics by an enhanced permeation and retention (EPR) effect. The polymeric micelle is one of the most successful drug delivery carriers because of their small size, high drug loading, prolonged blood circulation, and selective tumor accumulation. Therefore, in the present study, we selected a block copolymer of poly (ethylene glycol) (PEG) and poly (lactic acid) (PLA) (PEG-PLA) as the drug delivery system. Furthermore, we selected folic acid as an active targeting molecule to enhance the tumor-targeting effect. Folic acid can conjugate with folate receptor (FR), which is overexpressed in many types of tumors including ovarian,⁸ endometrial,⁹ breast,¹⁰ renal cell carcinomas,¹¹ and so forth. Targeting the folate receptor has shown considerable promise in mediating uptake of a variety of drugs, gene therapy products, and radiopharmaceuticals.¹²⁻¹⁴

Therefore, we have explored a new folic acid-conjugated PEG-PLA micelle delivery system for HB (HB/FA-PEG-PLA micelle). In the present study, the stability and drug release of the HB/FA-PEG-PLA micelles either *in vitro* or *in vivo* were studied. Tumor targeting effect and antitumor efficiency of the micelles *in vitro* were then evaluated. Furthermore, a mouse ovarian ascitic tumor model was established, and a pharmacokinetic study and tissue biodistribution of the HB/FA-PEG-PLA micelles were evaluated *in vivo* to further confirm their targeting effect. The results of our study showed that the new drug delivery system HB/FA-PEG-PLA micelles had prominently improved biocompatibility, prolonged blood circulation of HB, and had better targeting and antitumor effect against ovarian cancer.

2 | MATERIALS AND METHODS

2.1 | Materials

Lactide, diethyl ether, acetonitrile, methanoic acid, tetrahydrofuran (THF), MTT, hypocrellin B (HB), DMSO, *N*-hydroxysuccinimide (NHS), dicyclohexylcarbodiimide (DCC), potassium bis (trimethylsilyl) amide (KHMDs), epoxyethane (EO), 10% pluronic-68 (F-68), folic acid (FA) and DAPI were purchased from Fule Biological Technology Co., Ltd (Jinan, China). All human ovarian carcinoma cell lines were obtained

from the laboratory of Qilu Hospital, Shandong University (Jinan, China). FBS, RPMI-1640 and pancreatin were purchased from Kunteng Biological Technology Co., Ltd (Shandong, China); TRIzol reagent was supplied by Pufei (Shanghai, China); SYBR Green Master Mix was purchased from Takara Biotechnology Co., Ltd (Shanghai, China).

2.2 | Preparation of PEG-PLA and FA-PEG-PLA copolymer

PEG-PLA block copolymer was synthesized as described elsewhere.¹⁵ Recrystallized lactide (10 g) was added to a vial in argon gas. Then, THF (20 mL), KHMDs (1.5 mL) (initiator), and epoxyethane (2.4 mL) were added to another vial and stirred continuously for 2 days in an ice bath. Subsequently, the solutions of the 2 vials were mixed and stirred for 2 hours at 25°C. Anhydrous acetic acid (20 mL) was then added to the vial and stirred for 30 minutes at 25°C. Finally, 0.2 mL HCl was added to end the reaction; the PEG-PLA copolymer was well prepared. Folate (1 g) and DMSO (30 mL) were added into thea bottle (50 mL), and then added 0.9 g NHS and, 0.5 g DCC in were added in turn, stirred away from light for 12 hours at 30°C, and then filtering out of 1,3-dicyclohexylurea (DCU). Added Tthe filtrate and the PEG-PLA (1 g) were added to another bottle (50 mL), and then adjust the pH was adjusted to 8 with triethylamine, and lucifugal reaction for 24 hours at 30°C was carried out °C, which werewas dialyzed by a dialysis belt (2000 KkDa) in distilled water for 7 days 72 hours to remove the residual organic solvent and unincorporated folic acid. Attachment of the FA peptide and PEG-PLA was achieved by means of the hydroxyl groups of the FA peptides and the N-terminal groups on the surface of nanoparticles combining covalently.

2.3 | Preparation of drug-loaded micelles

The solvent evaporation method was used to load HB into the PEG-PLA diblock copolymer micelles. Briefly, 30 mg diblock copolymer was added to a vial containing 1.3 mL THF and homogenized by sonication for 5 minutes. HB in THF (200 µL; 2 mg/mL) was subsequently added to the vial and mixed uniformly. Then the mixture solutions of HB and PEG-PLA in THF were dropped into 20 mL of purified water maintained under vigorous magnetic stirring, then stirred for 3 hours continuously to form the HB/PEG-PLA micelles, which were dialyzed by a dialysis belt (3500 kDa) overnight to remove the residual organic solvent and unincorporated drugs. HB/FA-PEG-PLA micelles were also prepared by this method except that the copolymer was substituted with a mixture of FA-PEG-PLA copolymer and PEG-PLA copolymer with weight ratio of 1:9. All the micelles were added to 2.5% F-68 to obtain the solid powder.

2.4 | HB/FA-PEG-PLA micelles characterization

HB/FA-PEG-PLA micelles were characterized for particle size, size distribution and surface charge. Particle hydrodynamic diameter and zeta potential (ZP) were determined by light scattering (Malvern Instruments Ltd, Malvern, UK). Transmission electron microscopy

(TEM; Tecnai G2F20 S-Twin Fei Company, Hillsboro, OR, USA) was used to determine morphology and surface characteristics.

To determine the amount of HB encapsulated in the micelles, HPLC was used. Chromatographic separation was achieved using a reverse-phase C18 column (150 × 4.6 mm, 5 μm pore size, Shimadzu VP-ODS, Beijing Shimadzu Medical Equipment Co., Ltd., Beijing, China), the mobile phase solution was acetonitrile/methanoic acid (65:35, v/v); column temperature 25°C; UV detection wavelength: 300 nm; velocity: 0.8 mL/min; quantity: 20 μL. Dried micelles (2 mg) were dissolved in THF (1 mL), then the supernatants were collected after centrifugation (18 800 g, 10 minutes), and dried by N₂. The dried drugs were redissolved in 1-mL mobile phase solution and analyzed by HPLC. Drug-loading coefficient (DL) and encapsulation ratio (ER) were calculated as follows:

$$\text{DL\%} = \frac{\text{weight of the drug in micelles}}{\text{weight of the feeding polymer and drug}} \times 100\%;$$

$$\text{ER\%} = \frac{\text{weight of the drug in micelles}}{\text{weight of the feeding drug}} \times 100\%.$$

Release study of the micelles was evaluated by the dialysis method. Briefly, different formulation solutions with the same HB were transferred into a dialysis bag respectively and immersed in 50 mL PBS under mechanical shaking (70 r.p.m.) at 37°C. The solution outside the dialysis bag was sampled and replaced with fresh buffer solution at defined times. HB concentrations were measured by HPLC.

2.5 | Determination of folate receptor α (FRα) expression in ovarian cell lines

A2780, SKOV3 and HO8910 cells (Short Tandem Repeat for A2780, SKOV3 and HO8910 cells are shown in Figures S1, S2 and S3) were cultured in RPMI 1640 medium with 10% (v/v) FBS and 1% (v/v) penicillin/streptomycin combination. Total RNA was isolated from the above cells using TRIzol reagent, respectively. Qualitative RT-PCR was carried out using Fast-Start Universal SYBR Green Master Mix. Primers for FR gene expression detection were 5'-GAACGCCAAGCACCACAAG-3' (forward) and reverse: 5'-GGTCGACACTGCTCATGCAA-3' (reverse). Data analysis was carried out using the comparative Ct method (2^{ΔΔC_t}).

2.6 | Cell uptake of HB/FA-PEG-PLA micelles by fluorescence microscopy

Three types of cell lines were placed into 24-well tissue culture plates for 2 days, then washed twice with PBS and treated with 1 mL fresh serum-free medium containing HB/FA-PEG-PLA micelles, HB/PEG-PLA micelles, or free HB (HB concentration of 10 mg/mL). After 4-hour incubation at 37°C, each dish was rinsed 3 times with 1 mL cold PBS and then DAPI was added to cells for 10-minute incubation. The cells were washed 3 times again with PBS buffer and were finally detected by a fluorescence microscope; fluorescence intensity was analyzed using Image J software (National Institutes of Health, Rockville, MD, USA).

2.7 | In vitro phototoxicity and dark toxicity

MTT assay was used to evaluate phototoxicity and dark toxicity of different micelles to SKOV3 cells. SKOV3 cells were seeded into 96-well plates at a density of 1 × 10⁴ cells per well and grown for 24 hours at 37°C, then rinsed with PBS and incubated with serum-free medium containing HB/FA-PEG-PLA micelles, HB/PEG-PLA micelles, HB alone, or blank FA-PEG-PLA micelles. HB concentrations ranged from 10 to 100 μg/mL (n = 8). After 24 hour incubation, the plates were/were not given visible light at 650 nm, 3 J/cm² for 10 minutes to detect the phototoxicity or the dark toxicity of cells. Three types of HB solution were removed and washed with PBS twice, incubated with 20 μL MTT (0.5 mg/mL) solution for 4 hours and then removed. DMSO (200 μL) was added to cells for 10 minutes, then measured at 490 nm. Results were shown as average cell viability and percentage of inhibition and calculated as follows:

$$\text{Average cell viability} = \frac{[(\text{OD}_{\text{treat}} - \text{OD}_{\text{blank}})]}{(\text{OD}_{\text{control}} - \text{OD}_{\text{blank}})} \times 100\%;$$

$$\text{Percentage of inhibition} = (1 - \frac{\text{absorbance of treatment}}{\text{absorbance of control}}) \times 100\%.$$

2.8 | Animal model

Female Sprague-Dawley rats and female athymic nude mice (5-6 weeks old) were purchased from Weitong Lihua, Inc. (Beijing, China), and treated according to the protocols approved by the ethical committee of Shandong University. Tumor-bearing mice were prepared by transplanting SKOV3 cells into the peritoneal cavity of mice.

2.9 | Pharmacokinetic study in vivo

Calibration curves of HB in serum and tissues were prepared using the HPLC method. Briefly, tumor-bearing mice were anesthetized with diethyl ether, and blood was collected with heparin-treated tubes, which was immediately centrifuged at 18 800 g for 15 minutes to obtain the plasma. Organs such as liver, spleen, kidney, lung, intestine, ovary, and tumor tissues were carefully removed and homogenized with physiological saline to obtain the tissue samples. Different HB concentration solutions (200 μL; 1, 2.5, 5, 10, 25, 50, 100, 200 and 400 μg/mL) were added to 100 μL of plasma and tissues samples, then vortexed and centrifuged at 14 000 rpm for 15 minutes. TNF was added to each supernatant and centrifuged for another 10 minutes. Finally, the supernatants were dried by N₂ and analyzed by HPLC.

Female Sprague-Dawley rats were divided into 3 groups: those given HB/FA-PEG-PLA micelles; those given HB/PEG-PLA micelles; or those given free HB by tail vein injection (HB concentration 10 mg/kg). After drug injection, rats in every group (3/group) were

anesthetized at predetermined time points (10, 20, 30 and 40 minutes, 1, 2, 4, 6, 12, 24, 36, 48 and 60 hours), and blood was collected from the tail vein into heparin-treated tubes. Concentration of HB in every sample was analyzed by HPLC as described earlier.

2.10 | Tissue biodistribution study in vivo

For tissue biodistribution studies, SKOV3 tumor-bearing female athymic nude mice were divided into 3 groups (18/group). Each group was given the same ip dose of different micelles or free HB, similar to the pharmacokinetic studies. Three mice from each group were anesthetized at predetermined time points (1, 2, 4, 6, 12 and 24 hours), and blood and tissue samples were collected as described above. Concentrations of HB in blood and tissue samples were determined using a calibration curve by HPLC.

2.11 | Statistical analyses

Statistical evaluations of data were carried out by two-tailed Student's *t* test. Data are expressed as mean \pm SD. *P* < .05 was considered significant.

3 | RESULTS

3.1 | Preparation and characterization of HB/FA-PEG-PLA micelles

Chemical synthesis diagram of PEG-PLA-M is shown in Figure 1A, and the composition flowchart of HB/PEG-PLA-M and HB/FA-PEG-PLA-M is shown in Figure 1B. In ^1H NMR spectroscopic studies, FA-PEG-PLA copolymers had an obvious peak at 7.55 ppm, indicating that folic acid was successfully conjugated into the copolymer (Figure 1C). Confirmation of HB/FA-PEG-PLA micelles was determined using TEM (Figure 1D), which showed that the micelles have a smooth surface and spherical shape. HB/FA-PEG-PLA micelles were prepared with a narrow size distribution (as shown in Figure 1E). HB/FA-PEG-PLA micelles have a mean diameter of 173.8 ± 3.2 nm, which was larger than that of HB/PEG-PLA micelles (153.7 ± 7.8 nm). The surface charge of the micelles was approximately -30 mV either in HB/FA-PEG-PLA micelles or in HB/PEG-PLA micelles. Encapsulation efficiency of HB/FA-PEG-PLA micelles was $92.3\% \pm 2.4\%$ and the loading level was $4.5\% \pm 0.9\%$. Characterizations of both nano micelles are shown in Table 1.

The release profile of HB from 3 HB solutions under PBS was investigated (Figure 1F). The HB solution showed a limited burst release (21.9%) in PBS after 24 hours. After 160 hours, HB/FA-PEG-PLA-M and HB/PEG-PLA-M micelles and HB solution released an accumulated amount of HB of approximately $30.9\% \pm 0.9\%$, $29.2\% \pm 0.9\%$ and $45.5\% \pm 0.8\%$, respectively, which indicated that HB/FA-PEG-PLA micelles could not only solubilize poorly soluble HB, but also showed sustained drug release behavior.

3.2 | Cellular uptake of HB/FA-PEG-PLA micelles in vitro

As shown in Table 2, FR α mRNA was more strongly expressed in SKOV3 cells compared with HO8910 and A2780 cells. Therefore, we used SKOV3 cells of high FR expression in in vitro and in vivo studies. Figure 2 shows the uptake characteristics of HB/FA-PEG-PLA micelles, HB/PEG-PLA micelles and free HB solution in different cells. Fluorescence density of FA-conjugated micelles was much higher than that of free drug and plain micelles in all cell lines (*P* < .05) (Figure 2B). However, the fluorescence density of HB/PEG-PLA micelles was slightly higher than that of free HB solution, although there was no statistical significance (*P* > .05). For the 3 cell lines, fluorescence of HB/FA-PEG-PLA micelles in SKOV3 was significantly increased compared to that in HO8910 cells or A2780 cells (Figure 2C). HB/FA-PEG-PLA micelles in SKOV3 cell lines had the highest fluorescence density of 44.6 ± 2.6 compared to the other cell lines (*P* < .05).

3.3 | Phototoxicity and dark toxicity of HB/FA-PEG-PLA micelles in vitro

Cell viability rate of the PEG-PLA micelles without drug loading was very high, and they could reach $67.2\% \pm 2.2\%$ at a concentration as high as 100 $\mu\text{g}/\text{mL}$. Therefore, the unloaded micelles themselves had no toxicity to cells and were very safe for drug delivery. Table 3 shows that HB/FA-PEG-PLA micelles had higher cytotoxicities toward SKOV3 cells than that of plain HB micelles and free HB solution at all concentrations (*P* < .05) after photodynamic treatment. However, there was no statistically significant difference between plain HB micelles and free HB solution at most doses (*P* > .05). At the dose of 50 $\mu\text{g}/\text{mL}$ in particular, the inhibition rate of SKOV3 cells with HB/FA-PEG-PLA micelles was $69.5\% \pm 4.3\%$, which was 2-fold higher than that of plain micellar HB ($32.5\% \pm 9.6\%$) and free HB ($30.3\% \pm 5.6\%$) solution. The results indicated that FA-PEG-PLA micelles can enhance cytotoxicity of HB in SKOV3 cells on account of folate receptor-mediated internalization of micelles and amplification of the drug effect. Table 4 shows the dark toxicity of SKOV3 cells for 3 treatment groups, which indicated that there were no significant differences between the 3 groups at most doses (*P* > .05).

3.4 | Pharmacokinetic study in vivo

Linear regression equations between the concentration (*X*) and area under the curve (AUC) (*Y*) were established by linear regression analysis in blood and tissues (Figure 3). The established standard curve showed a good linear relationship in concentration ranging from 1 to 150 $\mu\text{g}/\text{mL}$ in either blood or tissues. These curves were used in the following pharmacokinetics and tissue distribution study in vivo.

HB/FA-PEG-PLA micelles and HB/PEG-PLA micelles showed remarkably prolonged blood circulation ($t_{1/2} = 13.5$ hours, 13.6 hours respectively) after iv dosage compared to free HB

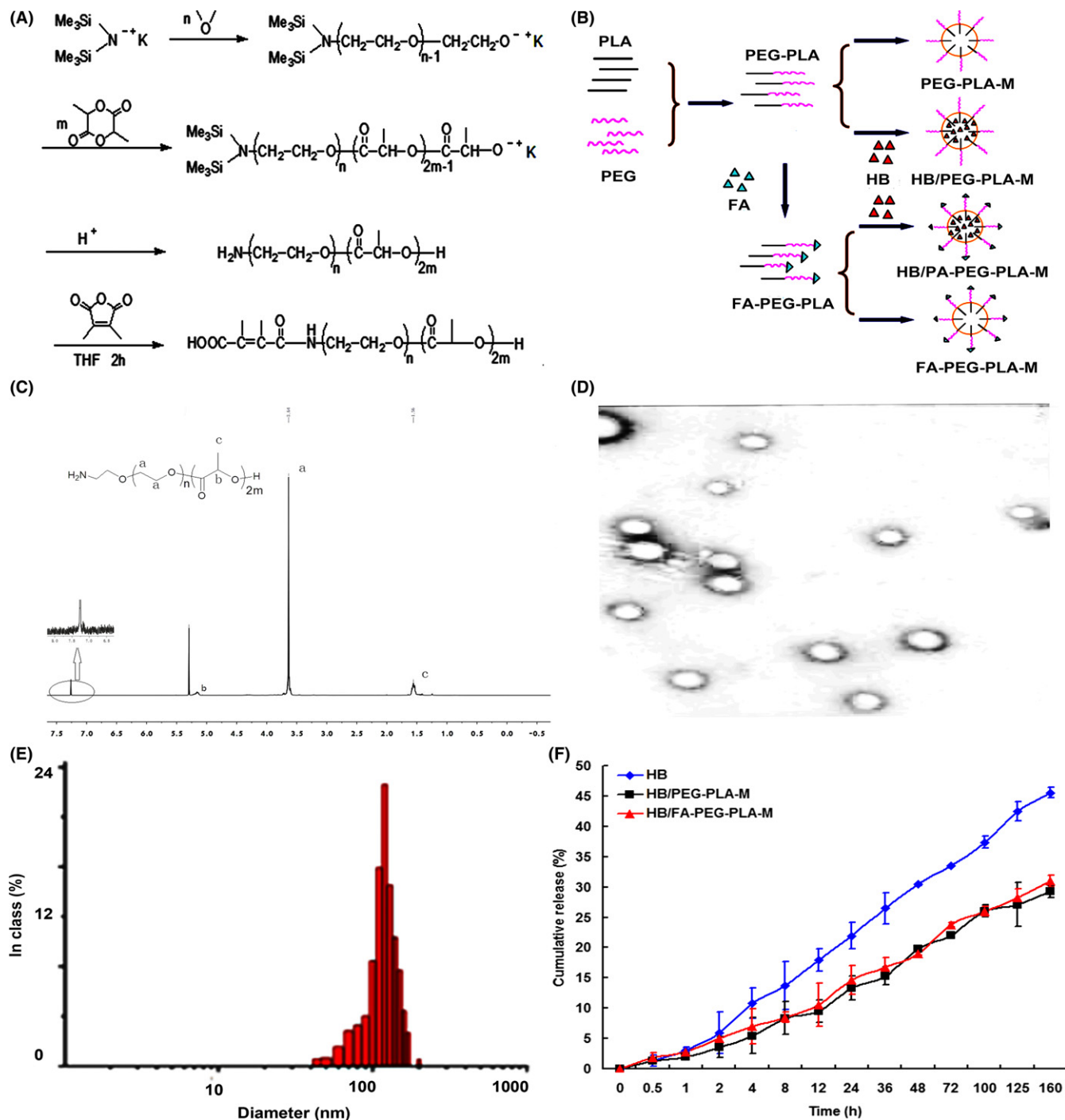


FIGURE 1 Characterization of hypocrelin B poly (ethylene glycol) (PEG)-poly (lactic acid)(PLA)-folate (HB/FA-PEG-PLA) micelles. A, Chemical synthesis diagram of PEG-PLA-M. B, Composition flowchart of HB/PEG-PLA-M and HB/FA-PEG-PLA-M. C, ^1H NMR image of PEG-PLA-FA-NP (nanoparticle). D, Transmission electron microscopy images of HB/FA-PEG-PLA-M. E, Particle size distribution pattern of HB/FA-PEG-PLA-M ($n = 5$). F, Release profile of HB from 3 formulations of HB solutions ($n = 5$)

($t_{1/2} = 7.4$ hours), as shown in Figure 4. Regarding HB/FA-PEG-PLA micelles, it was of interest that folate conjugation did not significantly affect the long-term circulation property of the micelles. AUC of HB/FA-PLG-PLA micelles and HB/PEG-PLA micelles was $355.25 \mu\text{g/mL}$ per hour and $338.53 \mu\text{g/mL}$ per hour, respectively, whereas AUC of free HB was $123.34 \mu\text{g/mL}$ per hour. These results were similar to the *in vitro* study, which further confirmed that

micelles provided remarkably prolonged blood circulation and enhanced accumulation of HB in blood.

3.5 | Biodistribution study *in vivo*

Distributions of the micelles in major organs after ip injection were studied. As shown in Figures 5 and 6, peak time of both micelles

TABLE 1 Characterizations of 2 nano micelles

Characterization	HB/PEG-PLA-M	HB/FA-PEG-PLA-M
Nanoparticle size	153.7 ± 7.8 nm	173.8 ± 3.2 nm
Zeta potential	-31.3 ± 1.3 mV	-34.9 ± 2.6 mV
Encapsulation efficiency	89.7% ± 3.27%	92.3% ± 2.45%
Loading level	8.3% ± 1.4%	4.5% ± 0.9%

FA-PEG-PLA, poly (ethylene glycol) (PEG)-poly (lactic acid)(PLA)-folate; HB, hypocrelin B.

was 6 hours in all tissues, which was much slower than that of free drug (4 hours). In the case of free HB, drug concentration decreased rapidly with time and was detected in a much lower concentration at the 24-hour sampling in each tissue, compared to the micelles. This observation suggests that both micelles have a much slower release and longer tissue retention for HB. In ovarian tumors shown in Figure 5F, concentrations of the folate-conjugated micelles HB/FA-PEG-PLA were 47.8 ± 1.5 µg/g, 49.6 ± 1.7 µg/g, 43.1 ± 0.9 µg/g, and 25.4 ± 1.4 µg/g at the 2nd, 6th, 12th and 24th hour, respectively; whereas with free HB, the concentration were much lower (i.e., 17.8 ± 0.9 µg/g, 25.9 ± 1.7 µg/g, 25.7 ± 1.7 µg/g, and 22.0 ± 0.9 µg/g respectively). Most noticeably, HB/FA-PEG-PLA micelles tended to accumulate in ovarian tumor 2.2- and 1.9-fold more than plain micelles and free HB, respectively, at the peak time point. On the contrary, the concentrations of plain micelles localized in tumors were similar to those of free HB at their peak time point (6 hours). These results indicated the higher retention potential and active targeting action of HB/FA-PEG-PLA micelles at the tumorous site, thereby enhancing therapeutic efficacy.

In most tissues, accumulations of folate-conjugated micelles were much higher than those of plain micelles and free drugs, as shown in Figure 7. Especially in kidney, HB/FA-PEG-PLA micelles were found to have much greater access to kidney, compared to the other 2 drug formulations. This observation suggests that kidney may be the major clearance organ for micelle systems and the bioactivity accounts for the higher concentration there. In contrast, free HB in liver was 413.3 ± 1.8 µg/g at peak, which was much higher compared to the micelles. The lower uptake of the micelles in the liver

may be attributed to PEGylation of polymer, which can decrease the uptake of nanoparticles by the reticuloendothelial system in the liver.

4 | DISCUSSION

Photodynamic therapy is a novel and promising therapy for advanced-stage ovarian cancer which is uncontrolled by routine treatment. The first key process in PDT therapy is the accumulation of photosensitizers in tumor tissues. To gain good aqueous solubility and high selectivity for the tumor, in the present study, we developed a novel active targeted system, FA-PEG-PLA copolymer micelles, to deliver HB.

An ideal targeted anticancer drug delivery system should have characteristics such as avoiding uptake by the reticuloendothelial system (RES), EPR, and active tumor-targeting.¹⁶⁻¹⁸ As a novel drug delivery system, FA-PEG-PLA copolymer has several advantages. First, the copolymer PEG-PLA micelles have the advantages of small size, high drug loading, and good biocompatibility. Second, PEG chain shell have an effective protein resistant property, which have the characteristic of steric repulsion effect, thus PEG could circumvent the uptake of RES. Also, the folate receptor is highly overexpressed in a number of human tumors including ovarian,¹⁹ breast, lung, brain, and renal cell cancers.²⁰⁻²² Third, we selected folic acid as the targeting ligand, which is cheap, non-immunogenic, retains high binding affinity, and is stable in storage and in the circulation.²³ In this study, HB/FA-PEG-PLA micelles showed a prolonged time for HB in the blood circulation, and better targeting and antitumor effect against ovarian cancer.

The drug release study in vitro showed that both micelles were released slower than the free HB group. Meanwhile, the pharmacokinetic and biodistribution study in vivo showed similar results. The elimination phase ($t_{1/2,\beta}$) of HB/FA-PEG-PLA and HB/PEG-PLA was 13.5 ± 1.1 hours and 13.6 ± 2.3 hours, respectively; whereas $t_{1/2,\beta}$ of free HB was only 7.4 ± 1.2 hours ($P < .05$). Furthermore, in tumor-bearing mice, free HB rapidly reached its peak at the 2nd hour in every organ; however, the peak times of both micelles were

TABLE 2 FR α expression of ovarian cancer cell lines

Ovarian cancer cell line	GAPDH	FOLR1	ΔC_t	$-\Delta\Delta C_t$	$2^{-\Delta\Delta C_t}$	Expression abundance	SD
A2780	14.33	26.53	12.2	-0.037	0.975	1.001	0.051
	14.23	26.31	12.0	0.083	1.059		
	14.25	26.46	12.2	-0.047	0.968		
SKOV3	12.01	17.67	5.66	6.503	90.719	79.914	9.779
	11.93	17.82	5.89	6.273	77.350		
	11.86	17.86	6	6.163	71.672		
HO8910	14.2	20.23	6.03	6.133	70.197	66.705	5.233
	14.23	20.47	6.24	5.923	60.688		
	14.22	20.27	6.05	6.113	69.230		

FR α , folate receptor α .

$P = .03$ A2780 vs SKOV3; $P = .02$ A2780 vs HO8910; $P = .05$ SKOV3 vs HO8910.

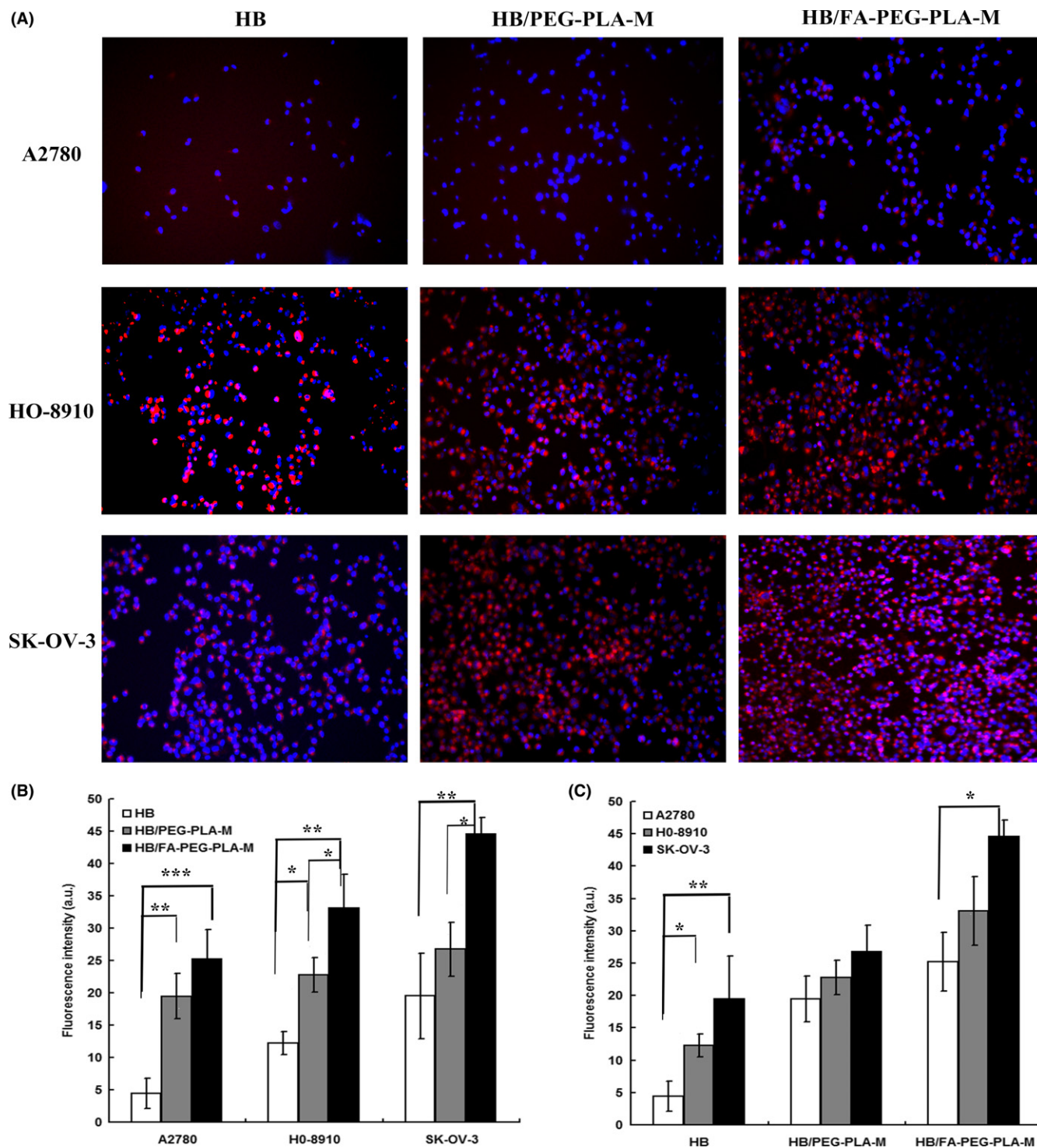


FIGURE 2 Uptake characteristics of hypocrellin B poly (ethylene glycol) (PEG)-poly (lactic acid)(PLA)-folate (HB/FA-PEG-PLA) micelles, HB/PEG-PLA micelles and free HB solution in different cells ($n = 8$). A, Cellular uptake of both micelles and free HB in SKOV3, HO8910, and A2780 cells by fluorescence microscopy. B/C, Fluorescence density half-qualitative analysis of HB/FA-PEG-PLA micelles, HB/PEG-PLA micelles and free HB groups in SKOV3, HO8910, and A2780 cells. $*P < .05$, $**P < .01$, $***P < .001$

postponed by at least 2 hours. As previously reported, the release mechanism of the PEG-PLA copolymer micelles is mainly diffusion-controlled release.²⁴ In our study, HB was dispersed in PLA polymers, which, inside the PEG membrane, was required to diffuse to the membrane surface first and then release successfully. Therefore,

the newly developed HB/FA-PEG-PLA micelles showed a well-controlled slow release for HB.

Selectivity of HB/FA-PEG-PLA micelles was well evaluated in vitro and in vivo. Fluorescence intensity of HB/FA-PEG-PLA micelles was much stronger than that of plain micelles and free HB

TABLE 3 Percentage of inhibition rates of SKOV3 cells after photodynamic treatment in different groups at different HB concentrations (n = 8)

Treatment	Concentration ($\mu\text{g/mL}$)				
	10	25	50	75	100
HB	20 \pm 3%	21 \pm 5%	30 \pm 6%	81 \pm 26%	96 \pm 6%
HB/PEG-PLA-M	16 \pm 2%	26 \pm 7%	32 \pm 9%	64 \pm 7%	86 \pm 8%
HB/FA-PEG-PLA-M	16 \pm 6%	36 \pm 9%	70 \pm 4%	96 \pm 10%	97 \pm 9%

FA-PEG-PLA, poly (ethylene glycol) (PEG)-poly (lactic acid)(PLA)-folate; HB, hypocrellin B.

in cells. Also, the higher the FR expressed in cells, the stronger the fluorescence density of HB/FA-PEG-PLA micelles. The strongest fluorescence density of HB/FA-PEG-PLA was in SKOV3 cells. In tumor-bearing mice, uptake of HB/FA-PEG-PLA micelles in tumors

TABLE 4 Dark toxicity (percentage of inhibition rates of SKOV3 cells) of blank nanoparticles and 3 other HB groups (n = 8)

Treatment	Concentration ($\mu\text{g/mL}$)				
	10	25	50	75	100
PEG-PLA-M	16 \pm 2%	23 \pm 4%	24 \pm 3%	28 \pm 5%	33 \pm 2%
HB	11 \pm 2%	28 \pm 7%	28 \pm 4%	31 \pm 2%	37 \pm 5%
HB/PEG-PLA-M	12 \pm 3%	26 \pm 6%	29 \pm 8%	32 \pm 4%	34 \pm 10%
HB/FA-PEG-PLA-M	14 \pm 1%	29 \pm 2%	34 \pm 6%	32 \pm 11%	39 \pm 9%

FA-PEG-PLA, poly (ethylene glycol) (PEG)-poly (lactic acid)(PLA)-folate; HB, hypocrellin B.

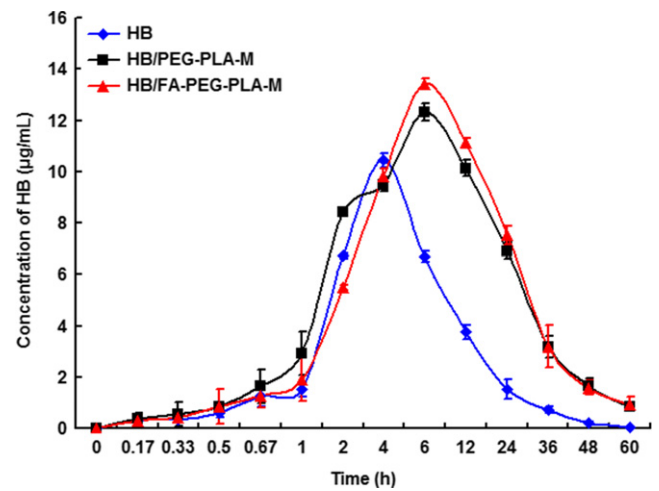


FIGURE 4 Pharmacokinetics features of different groups (n = 5). Hypocrellin B poly (ethylene glycol) (PEG)-poly (lactic acid)(PLA)-folate (HB/FA-PEG-PLA) micelles and HB/PEG-PLA micelles showed a remarkably prolonged blood circulation ($t_{1/2} = 13.5$ h, 13.6 h, respectively) compared to free HB ($t_{1/2} = 7.4$ h)

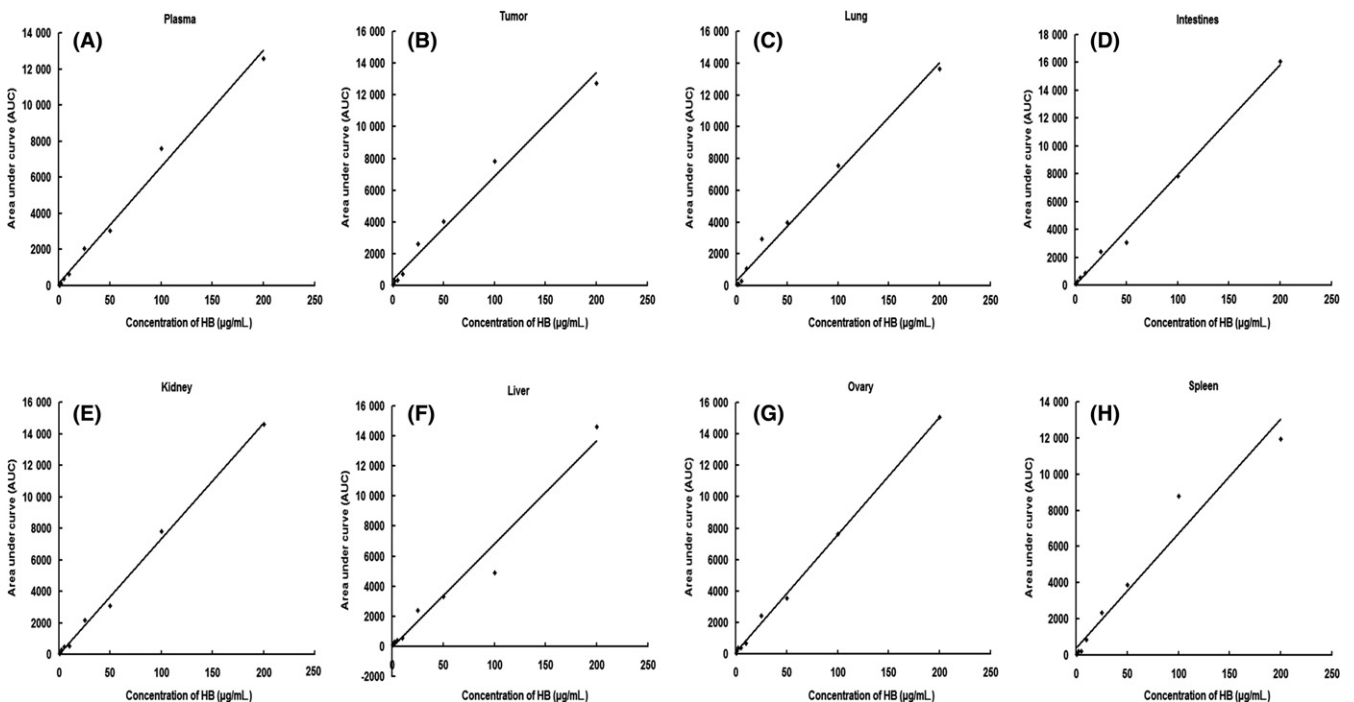


FIGURE 3 Established standard curve of plasma and tissues. A, plasma; B, tumor; C, lung; D, intestines; E, kidney; F, liver; G, ovary; H, spleen. HB, hypocrellin B

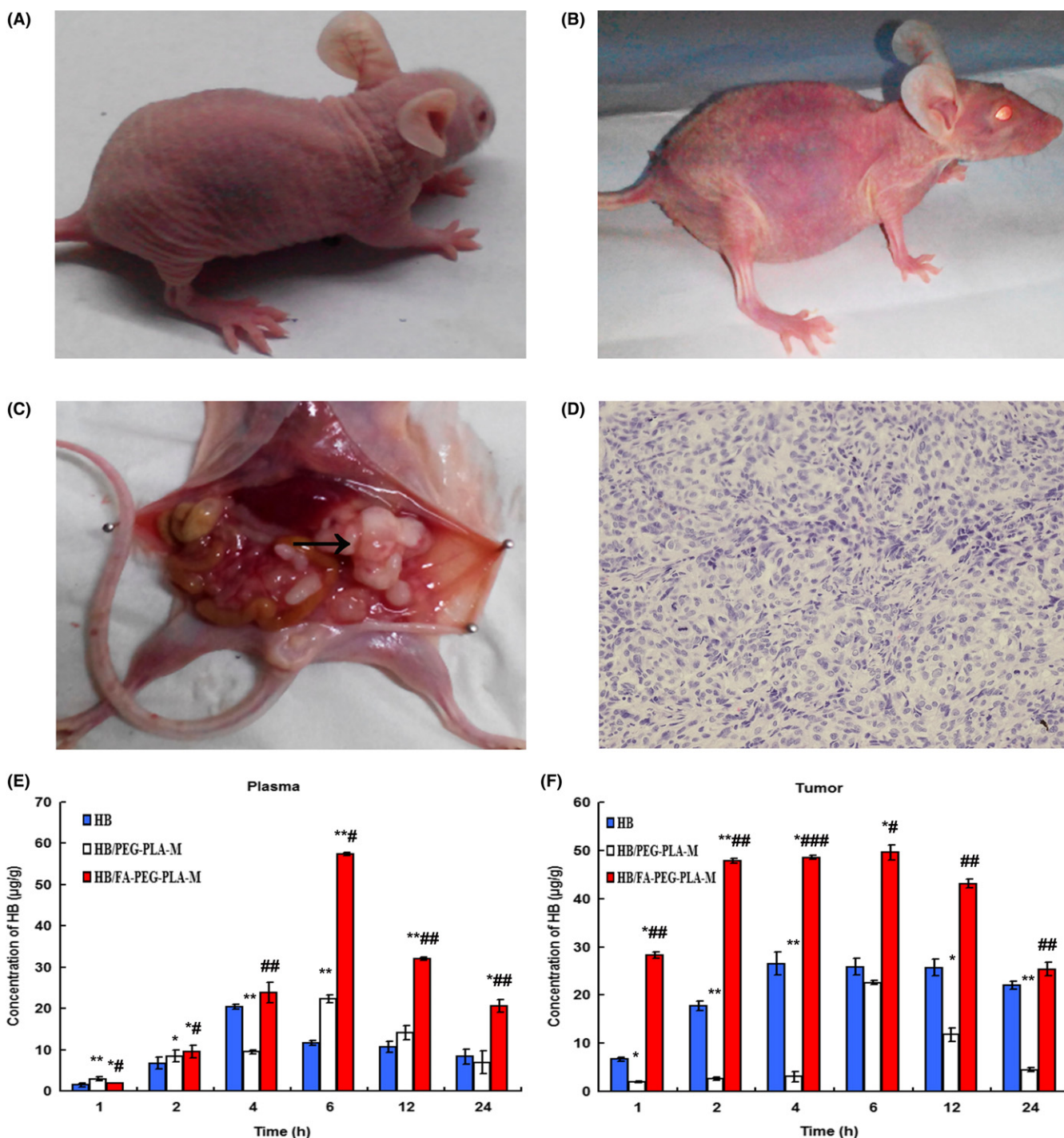


FIGURE 5 Tissue distributions of hypocrellin B (HB) in tumor tissues in different drug groups ($n = 3$). A, Normal animal. B, Tumor-bearing mouse model. C, Tumor tissues in abdominal cavity. D, H&E staining of abdominal tumor tissues. E, HB concentration of 3 groups in plasma. F, HB concentration of 3 groups in tumor tissues. * $P < .05$, ** $P < .01$ vs HB. # $P < .05$, ## $P < .01$, ### $P < .001$ vs HB/PEG-PLA-M. HB/FA-PEG-PLA, hypocrellin B poly (ethylene glycol) (PEG)-poly (lactic acid)(PLA)-folate

also rapidly reached a high level compared to other formulations, and the concentration of HB in HB/FA-PEG-PLA micelles was $47.8 \mu\text{g/g}$ 2 hours after ip injection, which was nearly 20-fold higher than that of HB in plain micelles ($2.7 \mu\text{g/g}$). Such a large shift in drug distribution is, after all, the result of a huge number of effective ligand-target interactions. After ip injection, plain micelles only

stagnate around the tumor tissues and cannot be taken up by tumors as a result of high molecular weight, reducing the actual drug concentration within the tumor. On the contrary, HB/FA-PEG-PLA micelles can be rapidly recognized by ligand-receptor interactions in tumors and deliver a much higher amount of HB to the tumor. As a result, HB/FA-PEG-PLA micelles have high selective targeting for

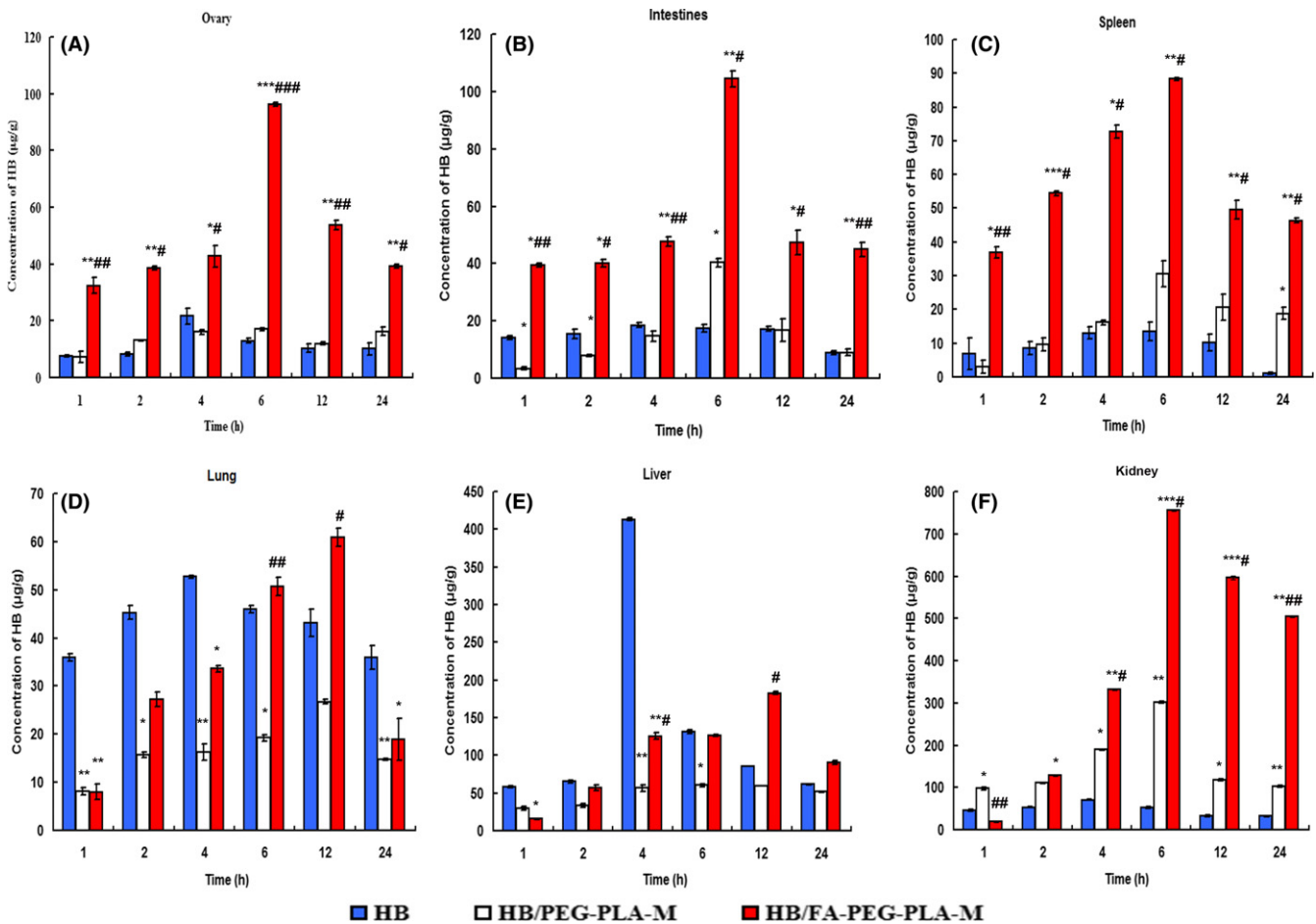


FIGURE 6 Distributions of micelles in major organs ($n = 3$). A, ovary; B, intestines; C, spleen; D, lung; E, liver; F, kidney. Peak times of both micelles was 6 h in all tissues, which was much slower than that of free drug (2 h). * $P < .05$, ** $P < .01$, *** $P < .001$ vs hypocrellin B (HB). # $P < .05$, ## $P < .01$, ### $P < .001$ vs HB/PEG-PLA-M. HB/FA-PEG-PLA, hypocrellin B poly (ethylene glycol) (PEG)-poly (lactic acid)(PLA)-folate

ovarian tumors. Moreover, the cytotoxicity of HB/FA-PEG-PLA micelles was dramatically stronger than that of plain micelles and free HB until the concentration of HB reached 100 µg/mL ($P < .05$), which further confirmed the targeting effect of FA-conjugated micelles. In contrast, plain micelles and free drugs showed no difference in the inhibitory rate of SKOV3 cells ($P > .05$). Therefore, HB/FA-PEG-PLA micelles have good selective targeting for ovarian tumors and enhanced the antitumor effect towards ovarian tumors.

In the present study, we used ip injection instead of iv injection. An ip dose of drug can yield higher drug concentrations and longer drug retention in the peritoneal cavity and in the peritoneal tissues, compared to an intravenous dose of the same formulation. Thus, ip therapy is confirmed as a good targeting method for ovarian cancer located in the peritoneal cavity. We systematically analyzed biodistributions of the newly developed HB/FA-PEG-PLA micelles by ip injection. As shown in Figure 6, nearly all formulations of the drugs were primarily confined to tissues and organs in the peritoneal cavity after ip dosage. Concentrations of HB in HB/FA-PEG-PLA micelles in most organs were much higher than that of plain micelles and free HB at all times. Tsai et al showed that the drug

uptake mechanism of peritoneal organs in the form of carriers by ip injection was passive diffusion and direct absorption into the organs.²⁵ Therefore, the EPR effect seems to have little effect on the uptake of drug carriers after ip injection. On the contrary, high affinity of folate ligand to FR expressed in organs is the major factor in determining the accumulation of drug carriers in peritoneal organs. This is the main reason that HB/FA-PEG-PLA micelles have greater accumulation in organs compared to the other 2 formulations. Our data showed that the kidney and liver, which had highly expressed FR, have much more accumulation of HB/FA-PEG-PLA micelles than other peritoneal organs, further confirming the above viewpoint. Accumulation of HB/FA-PEG-PLA micelles in tumors nearly reached a peak 2 hours after ip injection, whereas it took at least 6-12 hours to reach the peak of drug concentration in other peritoneal organs, as shown in Figure 7. This huge time difference will give us a chance to reduce cytotoxicity to normal tissues. In other words, we can give a green light at 2 hours after ip injection, which can effectively destroy tumor tissues as well as maximally reduce toxic side-effects to normal tissues.

Conclusively, our newly developed drug-delivery system of HB/FA-PEG-PLA micelles have prominently improved

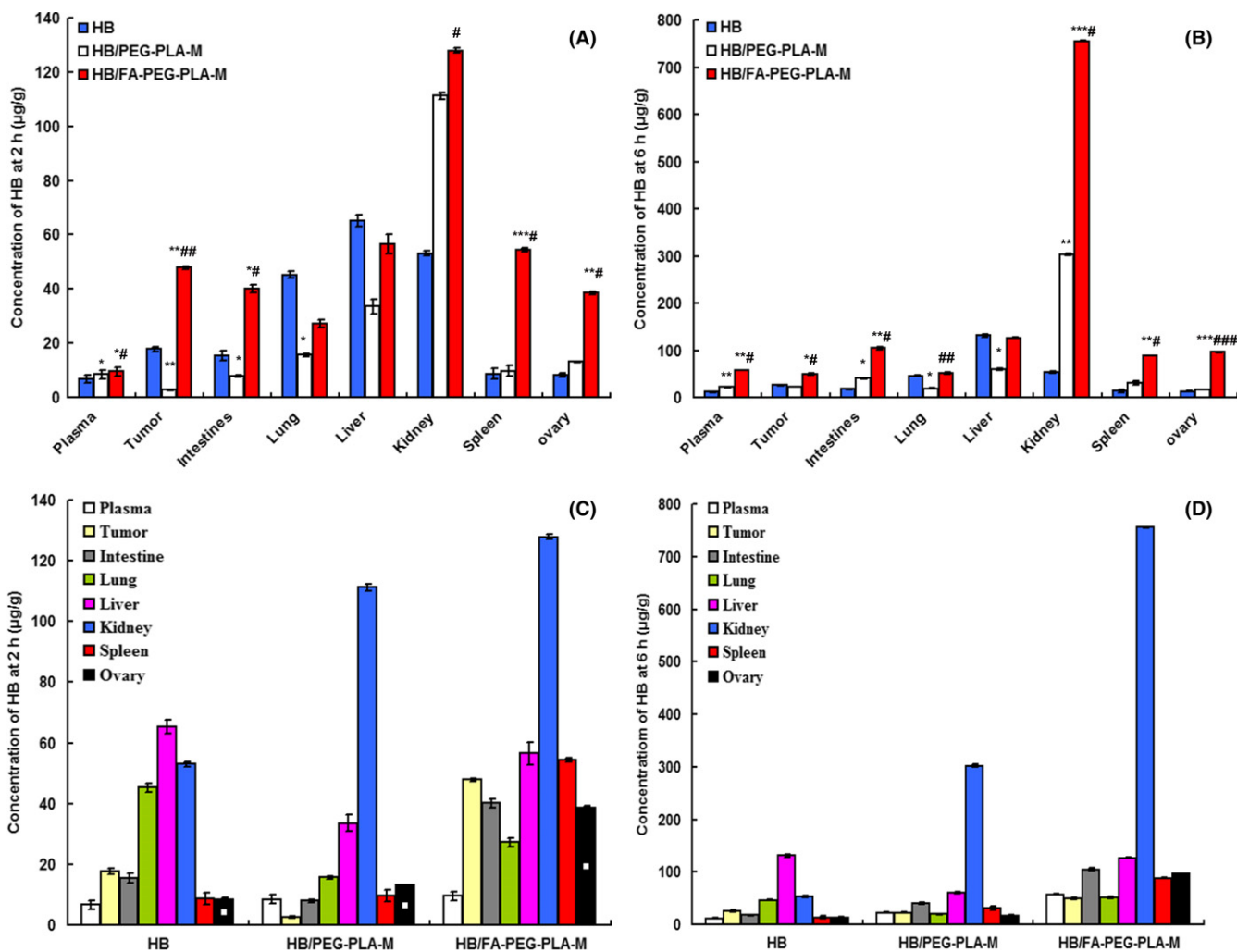


FIGURE 7 Distributions of micelles in blood, tumor tissues, and major organs at 2 and 6 h after drug delivery ($n = 3$). A, Drug distribution in different tissues at 2 h after drug delivery; B, the drug distribution in different tissues at 6 h after drug delivery; C, the drug distribution of three HB micelles in different tissues at 2 h after drug delivery; D, the drug distribution of three HB micelles in different tissues at 6 h after drug delivery. In each organ, hypocrellin B (HB) concentration was significantly higher in the order of FA-PEG-PLA, PEG-PLA, and free HB, except in the liver and lung. Kidney may be the major clearance organ. Accumulation of HB/FA-PEG-PLA micelles in tumors nearly reached the peak after 2 h, whereas it took at least 6 h to reach the peak in other peritoneal organs. * $P < .05$, ** $P < .01$, *** $P < .001$ vs HB. # $P < .05$, ## $P < .01$, ### $P < .001$ vs HB/PEG-PLA-M. HB/FA-PEG-PLA, hypocrellin B poly (ethylene glycol) (PEG)-poly (lactic acid)(PLA)-folate

biocompatibility, prolonged blood circulation of HB, and have better targeting and antitumor effect against ovarian cancer. In particular, the combination of HB/FA-PEG-PLA micelles and ip dosage shows promising results in terms of targeting efficacy, which will provide a new opportunity for the therapy of advanced-stage ovarian cancer. Further efforts to confirm the antitumor effect of this delivery system in vivo will be warranted in our future study.

ACKNOWLEDGMENTS

The authors acknowledge Shandong University and the Gynecological Tumor Laboratory for providing laboratory facilities and funds for this research. This work was supported by grants from the National Science Foundation of China (81172488) and the National Science Foundation of Shandong Province (ZR2016HB14).

CONFLICTS OF INTEREST

Authors declare no conflicts of interest for this article.

ORCID

Kun Song  <http://orcid.org/0000-0001-6110-2770>

REFERENCES

- Jessmon P, Boulanger T, Zhou W, Patwardhan P. Epidemiology and treatment patterns of epithelial ovarian cancer. *Expert Rev Anticancer Ther.* 2017;17:427-437.
- Azais H, Estevez JP, Foucher P, Kerbage Y, Mordon S, Collinet P. Dealing with microscopic peritoneal metastases of epithelial ovarian cancer. A surgical challenge. *Surg Oncol.* 2017;26:46-52.

3. Vilos C, Morales FA, Solar PA, et al. Paclitaxel-PHBV nanoparticles and their toxicity to endometrial and primary ovarian cancer cells. *Biomaterials*. 2013;34:4098-4108.
4. Zhang L, Zhu D, Dong X, et al. Folate-modified lipid-polymer hybrid nanoparticles for targeted paclitaxel delivery. *Int J Nanomedicine*. 2015;10:2101-2114.
5. Mondal G, Kumar V, Shukla SK, Singh PK, Mahato RI. EGFR-targeted polymeric mixed micelles carrying gemcitabine for treating pancreatic cancer. *Biomacromol*. 2016;17:301-313.
6. Nishiyama N, Matsumura Y, Kataoka K. Development of polymeric micelles for targeting intractable cancers. *Cancer Sci*. 2016;107:867-874.
7. Kim S, Lee DJ, Kwag DS, Lee UY, Youn YS, Lee ES. Acid pH-activated glycol chitosan/fullerene nanogels for efficient tumor therapy. *Carbohydr Polym*. 2014;101:692-698.
8. Walters CL, Arend RC, Armstrong DK, Naumann RW, Alvarez RD. Folate and folate receptor alpha antagonists mechanism of action in ovarian cancer. *Gynecol Oncol*. 2013;131:493-498.
9. Senol S, Ceyran AB, Aydin A, et al. Folate receptor alpha expression and significance in endometrioid endometrium carcinoma and endometrial hyperplasia. *Int J Clin Exp Pathol*. 2015;8:5633-5641.
10. Leone JP, Bhargava R, Theisen BK, Hamilton RL, Lee AV, Brufsky AM. Expression of high affinity folate receptor in breast cancer brain metastasis. *Oncotarget*. 2015;6:30327-30333.
11. Assaraf YG, Leamon CP, Reddy JA. The folate receptor as a rational therapeutic target for personalized cancer treatment. *Drug Resist Updat*. 2014;17:89-95.
12. Tong LX, Chen W, Wu J, Li HX. Folic acid-coupled nano-paclitaxel liposome reverses drug resistance in SKOV3/TAX ovarian cancer cells. *Anticancer Drugs*. 2014;25:244-254.
13. Kwon OJ, Kang E, Choi JW, Kim SW, Yun CO. Therapeutic targeting of chitosan-PEG-folate-complexed oncolytic adenovirus for active and systemic cancer gene therapy. *J Control Release*. 2013;169:257-265.
14. Ocak M, Gillman AG, Bresee J, et al. Folate receptor-targeted multimodality imaging of ovarian cancer in a novel syngeneic mouse model. *Mol Pharm*. 2015;12:542-553.
15. Yao S, Li L, Su XT, et al. Development and evaluation of novel tumor-targeting paclitaxel-loaded nano-carriers for ovarian cancer treatment: in vitro and in vivo. *J Exp Clin Cancer Res*. 2018;37:29. <https://doi.org/10.1186/s13046-018-0700-z>
16. Fang Z, Wan LY, Chu LY, Zhang YQ, Wu JF. 'Smart' nanoparticles as drug delivery systems for applications in tumor therapy. *Expert Opin Drug Deliv*. 2015;12:1943-1953.
17. Maeda H, Nakamura H, Fang J. The EPR effect for macromolecular drug delivery to solid tumors: improvement of tumor uptake, lowering of systemic toxicity, and distinct tumor imaging in vivo. *Adv Drug Deliv Rev*. 2013;65:71-79.
18. Jain V, Jain S, Mahajan SC. Nanomedicines based drug delivery systems for anti-cancer targeting and treatment. *Curr Drug Deliv*. 2015;12:177-191.
19. Wen YF, Graybill WS, Previs RA, et al. Immunotherapy targeting folate receptor induces cell death associated with autophagy in ovarian cancer. *Clin Cancer Res*. 2015;21:448-459.
20. Zhang Z, Wang J, Tacha DE, et al. Folate receptor alpha associated with triple-negative breast cancer and poor prognosis. *Arch Pathol Lab Med*. 2014;138:890-895.
21. O'Shannessy DJ, Yu G, Smale R, et al. Folate receptor alpha expression in lung cancer: diagnostic and prognostic significance. *Oncotarget*. 2012;3:414-425.
22. Liu X, Ma S, Yao Y, et al. Differential expression of folate receptor alpha in pituitary adenomas and its relationship to tumor behavior. *Neurosurgery*. 2012;70:1274-1280.
23. Ferrari R, Lupi M, Colombo C, Morbidelli M, D'Incalci M, Moscatelli D. Investigation of size, surface charge, PEGylation degree and concentration on the cellular uptake of polymer nanoparticles. *Colloids Surf B Biointerfaces*. 2014;123:639-647.
24. Xiao RZ, Zeng ZW, Zhou GL, Wang JJ, Li FZ, Wang AM. Recent advances in PEG-PLA block copolymer nanoparticles. *Int J Nanomed*. 2010;5:1057-1065.
25. Tsai M, Lu Z, Wang J, Yeh TK, Wientjes MG, Au JL. Effects of carrier on disposition and antitumor activity of intraperitoneal Paclitaxel. *Pharm Res*. 2007;24:1691-1701.

SUPPORTING INFORMATION

Additional supporting information may be found online in the Supporting Information section at the end of the article.

How to cite this article: Li J, Yao S, Wang K, et al. Hypocrellin B-loaded, folate-conjugated polymeric micelle for intraperitoneal targeting of ovarian cancer in vitro and in vivo. *Cancer Sci*. 2018;109:1958-1969. <https://doi.org/10.1111/cas.13605>